

<https://doi.org/10.1038/s41541-025-01150-9>

# TnSeq identifies genetic requirements of *Mycobacterium tuberculosis* for survival under vaccine-induced immunity



Kimra S. James<sup>1</sup>, Neharika Jain<sup>2</sup>, Kelly Witzl<sup>1</sup>, Nico Cicchetti<sup>1</sup>, Sarah M. Fortune<sup>3</sup>, Thomas R. Ioerger<sup>4</sup>, Amanda J. Martinot<sup>2</sup>✉ & Allison F. Carey<sup>1</sup>✉

*Mycobacterium tuberculosis* (Mtb), the etiologic agent of tuberculosis (TB), remains a persistent global health challenge due to the lack of an effective vaccine. The only licensed TB vaccine, Bacille Calmette-Guerin (BCG), is a live attenuated strain of *Mycobacterium bovis* that protects young children from severe disease but fails to provide protection through adulthood. It is unclear why BCG provides incomplete protection despite inducing a robust Th1 immune response. We set out to interrogate mycobacterial determinants of vaccine escape using a functional genomics approach, TnSeq, to define bacterial genes required for survival in mice vaccinated with BCG, the live attenuated Mtb vaccine strain,  $\Delta$ LprG, and in mice with Mtb immunity conferred by prior infection. We find that critical virulence genes associated with acute infection and exponential growth are less essential in hosts with adaptive immunity, including genes encoding the Esx-1 and Mce1 systems. Genetic requirements for Mtb growth in vaccinated and previously Mtb-infected hosts mirror the genetic requirements reported for bacteria under in vitro conditions that reflect aspects of the adaptive immune response. Across distinct immunization conditions, differences in genetic requirements between live attenuated vaccines and vaccination routes are observed, suggesting that different immunization strategies impose distinct bacterial stressors. Collectively, these data support the idea that Mtb requires genes that enable stress adaptation and growth arrest upon encountering the restrictive host environment induced by the adaptive immune response. We demonstrate that TnSeq can be used to understand the bacterial genetic requirements for survival in vaccinated hosts across pre-clinical live attenuated vaccines and therefore may be applied to other vaccine modalities. Understanding how Mtb survives vaccine-induced immunity has the potential to inform the development of new vaccines or adjuvant therapies.

*Mycobacterium tuberculosis* (Mtb), the etiologic agent of tuberculosis (TB), caused over 10 million infections in 2023, resulting in 1.25 million deaths across the globe<sup>1</sup>. One reason why TB remains a persistent global health challenge is the lack of an effective vaccine. The only licensed TB vaccine, Bacille Calmette-Guerin (BCG), is a live attenuated strain of *Mycobacterium bovis* developed over 100 years ago. BCG is effective in preventing severe, extrapulmonary TB disease in infants and young children, a major cause of morbidity and mortality in TB-endemic regions. However, BCG provides

minimal protection against pulmonary TB in adults, the most common form of the disease, despite inducing a durable memory response<sup>2</sup>.

It is unclear why BCG-induced immunity provides incomplete protection. BCG elicits a robust CD4<sup>+</sup> T-cell response, which, via IFN $\gamma$  production, enhances macrophage oxidative burst and phagolysosomal maturation, resulting in increased bacterial killing<sup>3</sup>. CD4<sup>+</sup> T cells also promote antibody production and maturation<sup>4</sup>, and recruitment and activation of cytotoxic CD8<sup>+</sup> T cells and other effector cells<sup>5,6</sup>. While IFN $\gamma$  production

<sup>1</sup>Division of Microbiology & Immunology, Department of Pathology, University of Utah, Salt Lake City, UT, USA. <sup>2</sup>Department of Infectious Disease and Global Health, Tufts University Cummings School of Veterinary Medicine, North Grafton, MA, USA. <sup>3</sup>Department of Immunology & Infectious Diseases, Harvard T.H. Chan School of Public Health, Boston, MA, USA. <sup>4</sup>Department of Computer Science and Engineering, Texas A&M University, College Station, TX, USA. ✉ e-mail: [amanda.martinot@tufts.edu](mailto:amanda.martinot@tufts.edu); [allison.carey@path.utah.edu](mailto:allison.carey@path.utah.edu)

is clearly necessary for vaccine-induced protection, the frequency of IFN- $\gamma$ -producing T cells in vaccinated individuals is not predictive of disease risk, suggesting that additional bacterial control mechanisms are involved<sup>7</sup>. In contrast to the intensive studies of the immune response induced by BCG vaccination, mycobacterial determinants of vaccine escape remain unknown, further hampering the rational design of improved immunization strategies. Understanding how Mtb survives in the setting of vaccine-induced immunity could uncover bacterial vulnerabilities that inform the development and prioritization of new vaccines or adjuvant therapies.

With the goal of uncovering such vulnerabilities, we used a functional genomics approach, TnSeq, to define mycobacterial genes required for survival in vaccinated mice and mice with immunity conferred by prior Mtb infection. TnSeq entails generating a genome-wide, saturated bacterial mutant library with a randomly integrating transposon, then selecting this library under a defined growth condition. Next-generation sequencing is used to map transposon insertion sites in input and output libraries, and the distribution of insertions across the genome is compared to identify genes with differences in insertion frequency. Genes with fewer transposon insertions in the output library are considered conditionally essential for bacterial growth, while genes with no change or an increase in insertion abundance are considered conditionally non-essential. Transposon mutagenesis has been used to define the genes mycobacteria require to survive under myriad *in vitro* and *in vivo* conditions, providing important insights into bacterial physiology<sup>8–20</sup>. We therefore reasoned that TnSeq could be used to understand how Mtb survives the numerous pressures imposed by the pathogen-specific adaptive immune response when applied in the context of vaccination and post-primary infection.

This pathogen-centric approach provided new insights into the physiology of Mtb under immune memory. Of note, we found that virulence genes required to establish acute infection, *Esx-1* and *Mce1*, are less essential in hosts with immune memory. Integrative analysis of our data with published TnSeq datasets suggests that the cellular microenvironment of the vaccine-induced immune response is more akin to what Mtb experiences during chronic infection, when bacterial growth becomes constrained. Defining the bacterial genetic requirements for survival in vaccinated hosts across pre-clinical live attenuated vaccines (LAV) may provide a more nuanced understanding of correlates and mechanisms of protection, and lead to improved vaccines to curb this ongoing global health emergency.

## Results

### Comprehensively defining *M. tuberculosis* genetic requirements for survival in BCG-vaccinated hosts

The added immune pressure conferred by BCG vaccination is expected to impose substantial selection against the bacterium during infection, yet the genes and pathways Mtb relies on to survive in this context remain largely unknown. We wished to define this suite of bacterial genes by performing TnSeq in BCG-vaccinated mice. Prior studies in the C57BL/6 mouse model have found that subcutaneous BCG vaccination confers ~0.5–1.5 log reduction in total Mtb burden<sup>21–24</sup>. To ensure that we would not bottleneck the complex pool of mutants in our transposon library with this selective pressure, we performed a preliminary study in mice that were aerogenically infected with a low dose (~100 CFU) of H37Rv. Because ongoing Mtb infection has been shown to impose near-sterilizing protection against secondary infection in non-human primates<sup>25</sup>, we reasoned that if the transposon library was not bottlenecked under this selective pressure, it would not be bottlenecked by BCG vaccination. We challenged the aerosol-infected and age-matched naïve C57BL/6 mice with a saturated transposon library generated in the widely used Mtb reference strain H37Rv<sup>11</sup>. Two and four weeks post-challenge, mice were sacrificed and tissue harvested for CFU enumeration and to recover genomic DNA from the surviving mutants for transposon-junction sequencing. Concomitant Mtb infection reduced bacterial burden by ~1.5 logs in the spleen, the site of transposon library selection, at these time points (Supplementary Fig. 1a). Transposon-junction sequencing and mapping of the surviving mutants with the Transit pre-processing software tool<sup>26</sup> found that approximately one third fewer

mutants survived in animals with ongoing Mtb infection as compared to naïve mice (Supplementary Data 1). This represents a moderate selection pressure comparable to the selection imposed on the input library by naïve C57BL/6 mice<sup>12</sup>, but less than that imposed in some antibiotic TnSeq screens<sup>27</sup>. Analysis of reproducibility between individual mice within each arm of the experiment revealed high correlation coefficients for mean transposon count across each gene (Spearman correlation coefficients 0.77–0.93, Supplementary Fig. 1b).

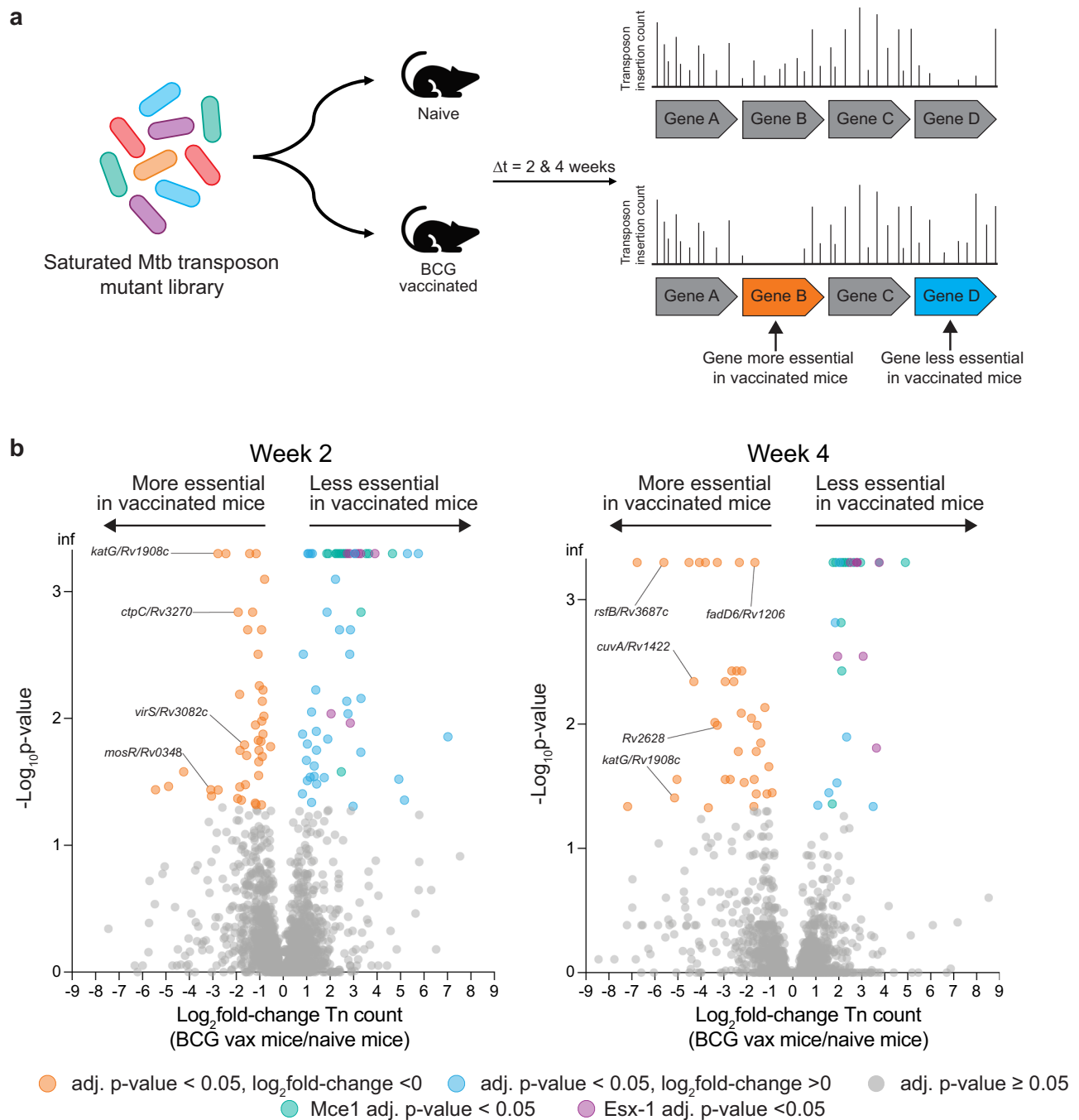
As there was no evidence of transposon library bottlenecking in mice with ongoing Mtb infection, we next challenged BCG-vaccinated and age-matched naïve C57BL/6 mice using the same approach (Fig. 1a). We found that subcutaneous BCG vaccination reduced total bacterial burden by ~1.5 logs at 2 and 4 weeks post-challenge (Supplementary Fig. 1c), consistent with prior studies. Selective pressure, as indicated by library saturation, was slightly less than that observed in our preliminary study, and reproducibility among animals was similarly high (Spearman correlation coefficients 0.76–0.93, Supplementary Fig. 1d). To identify genes that are differentially essential between naïve and BCG-vaccinated animals, we performed head-to-head comparisons of the output transposon libraries using the Transit resampling method<sup>28</sup>. With correction for multiple testing, we found that 102 genes were differentially essential 2 weeks post-challenge, and 64 genes were differentially essential 4 weeks post-challenge (adj. *p* value < 0.05, Fig. 1b, Supplementary Data 1).

Given the selective pressure imposed by vaccination, we expected to identify genes that were more essential in immunized relative to naïve mice. Consistent with this expectation, 41 genes had a statistically significant decrease in transposon insertion count in BCG-vaccinated mice compared to naïve mice 2 weeks post-challenge. The set of genes conditionally essential for survival in vaccinated mice are distributed across a number of functional categories, and pathway analysis did not identify significant enrichment in any category (Supplementary Fig. 2a). However, among the more essential genes are *katG/Rv1908c*, which encodes a catalase-peroxidase that detoxifies reactive oxygen species; *mosR/Rv0348*, a transcriptional regulator induced by hypoxia and one of the most highly expressed genes during chronic infection in mice; *virS/Rv3082c*, a pH-responsive transcriptional regulator activated in the phagolysosome; and *ctpC/Rv3270*, a P-type ATPase responsible for metalating *sodA*, the major superoxide dismutase in Mtb. Altogether, these genes represent responses to host-imposed stresses enhanced by BCG vaccination, such as the CD4<sup>+</sup> T-cell-mediated increase in IFN- $\gamma$  and TNF- $\alpha$  from infected and bystander macrophages<sup>29</sup>.

Four weeks post-challenge, 36 genes were significantly more required in vaccinated as compared to naïve mice. Only one gene, the catalase-peroxidase *katG/Rv1908c*, overlapped with the more essential genes at the 2-week time point (Supplementary Fig. 2a), suggesting continued, enhanced oxidative stress in vaccinated hosts. Among the other genes most essential for growth 4 weeks post-challenge are *rsfB/Rv3687c*, an anti-anti-sigma factor that enhances the activity of the alternative sigma factor  $\sigma^F$ , which plays a central role in stress response and persistence during chronic infection<sup>30</sup>; *cuvA/Rv1422*, which encodes a protein involved in lipid utilization and has a persistence defect when deleted<sup>31</sup>; *fadD6/Rv1206*, an acyl-CoA synthetase that promotes triacylglycerol accumulation and mycobacterial dormancy<sup>32</sup>; and *Rv2628*, a hypothetical protein in the DosR dormancy regulon that encodes an antigen associated with latent infection<sup>33,34</sup>. Altogether, many of these genes are linked to the induction and maintenance of Mtb dormancy, suggesting that Mtb's ability to arrest growth is critical to surviving the memory immune response.

### Canonical virulence genes are less required in BCG-vaccinated mice

Unexpectedly, approximately half of the statistically significant genes were less essential in BCG-vaccinated mice compared to naïve mice, displaying an increase in transposon insertion count: 61 genes two weeks post-challenge and 28 genes four weeks post-challenge (Fig. 1b, Supplementary Data 1). These two gene sets are highly overlapping, and pathway analysis found that the functional category “virulence” was significantly



over-represented at both time points (Supplementary Fig. 2b). Notably, many of the less essential genes belong to two systems that play key roles in Mtb pathogenesis and its intracellular lifestyle: the Esx-1 Type VII secretion system, and the Mce1 lipid uptake system (Figs. 1b and 2a, Supplementary Fig. 2b).

Both the Esx-1 and Mce1 systems are known to be essential for Mtb growth in vivo<sup>9,35–39</sup>. The Esx-1 system consists of a Type VII transmembrane secretion system and secreted effector proteins, which are critical to Mtb pathogenesis<sup>40</sup>. A key role of Esx-1 is to permeabilize the phagolysosomal membrane, facilitating release of bacterial components into the cytosol, thereby initiating a complex innate immune response from the host<sup>41–45</sup>. The Esx-1 secretion system, secreted proteins, and regulatory factors are encoded across two unlinked genomic loci<sup>40</sup>. Genes across both

loci were significantly less essential in BCG-vaccinated mice as compared to naïve mice at both time points (Fig. 2a, Supplementary Fig. 3a, Supplementary Data 1). Most genes in the Esx-1 loci that did not reach statistical significance showed a trend towards an increase in the number of transposon insertions (Fig. 2a, Supplementary Fig. 3a, Supplementary Data 1). Some short genes in the Esx-1 system, such as *esxA/Rv3875* and *esxB/Rv3874*, which encode the secreted proteins ESAT-6 and CFP-10, have few transposon insertion sites, making it difficult to reach statistical significance, a known limitation of TnSeq methodology.

Mce1 is also a transmembrane complex and is responsible for importing host-derived fatty acids, an important nutrient for Mtb during acute infection<sup>36</sup>. The Mce1 system is encoded across a 12-gene operon, with seven accessory genes distributed across the genome. All 12 of the genes in

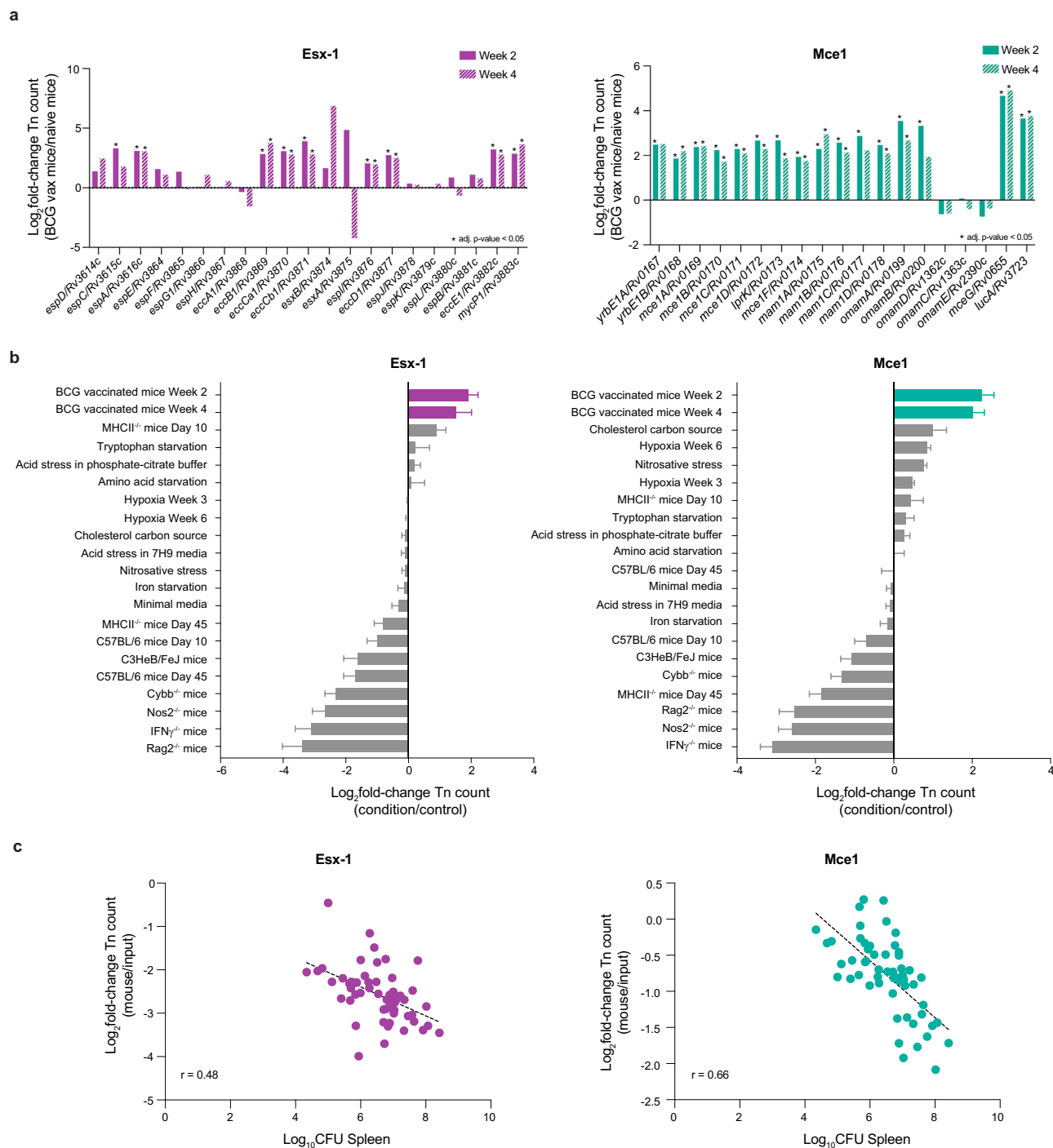


**Fig. 2 | Critical virulence genes are less essential in BCG-vaccinated mice.** **a** Log<sub>2</sub> fold-change in transposon read count for each gene in the Esx-1 system and Mce1 system in BCG-vaccinated mice relative to naïve mice. Asterisks indicate adj.  $p < 0.05$  by the Transit resampling pipeline, as detailed in the “Methods.” **b** Mean log<sub>2</sub> fold-change in transposon read count for genes in the Esx-1 or Mce1 systems across defined in vitro conditions and mouse genetic backgrounds. Error bars

represent SEM. Purple bars represent data from this study. Gray bars indicate data from the MtbTnDb database. **c** Correlation between log<sub>2</sub> fold-change in transposon read count averaged across Esx-1 or Mce1 genes and bacterial burden across a set of genetically diverse mouse backgrounds. Log<sub>2</sub> fold-change is relative to the input transposon library. Each dot represents one mouse background ( $n = 1$ –6 mice per background).

the Mce1 operon, in addition to the accessory genes *lucA/Rv3723*, *omamA/Rv0199*, *omamB/Rv0200*, and *mceG/Rv0655*, were significantly less essential in BCG-vaccinated mice compared to naïve mice at one or both time points (Fig. 2a, Supplementary Fig. 3a, Supplementary Data 1).

We note that the reduced essentiality of Esx-1 in BCG-vaccinated mice is relative, rather than absolute. Transposon insertions across the Esx-1 genes are increased in vaccinated compared to naïve mice. However, relative

to the input library, they are decreased (Supplementary Fig. 3b). By contrast, bacteria with transposon insertions across the Mce1 genes are more abundant in vaccinated mice as compared to the input library (Supplementary Fig. 3b), suggesting an absolute growth advantage for Mce1 mutants in vaccinated mice.

To validate our observation that the Esx-1 virulence system is less essential in vaccinated mice, we challenged groups of BCG-vaccinated and



naïve animals with either wild-type H37Rv or an *Esx-1* deletion mutant<sup>46</sup> (Supplementary Fig. 3c). Two and four weeks post-challenge, animals were sacrificed and CFU enumerated from the spleens and lungs. To quantify the relative fitness cost of *Esx-1* disruption in naïve compared to BCG-vaccinated animals, we calculated the  $\log_{10}$  difference in bacterial burden (CFU) between naïve and vaccinated animals. We found that the *Esx-1* deletion strain had a substantial growth defect in naïve mice 2 and 4 weeks post-infection, consistent with previous reports<sup>37,38,47</sup>. However, this growth defect was reduced in BCG-vaccinated mice in the spleen, with an even greater effect in the lung (Supplementary Fig. 3c). These results support our TnSeq findings that the *in vivo* essentiality of a canonical virulence system, *Esx-1*, is partially rescued in the context of BCG vaccination.

### Decreased essentiality of *Esx-1* and *Mce1* genes in vaccinated hosts corresponds to conditions promoting *Mtb* growth arrest

What does it mean for virulence systems to be less essential in vaccinated mice? To gain biological insight, we evaluated the requirement for *Esx-1* and *Mce1* genes across TnSeq datasets obtained from the MtbTnDb database<sup>48</sup>. MtbTnDb has aggregated data from TnSeq experiments across numerous growth conditions, and the raw sequencing data have been standardized and analyzed by Transit, the same pipeline used here. We extracted data from MtbTnDb for wild-type H37Rv transposon libraries selected under defined *in vitro* conditions or wild-type and knock-out mice for comparison to our data (Supplementary Data 2). We then plotted the mean  $\log_2$  fold-change in transposon read count averaged across *Esx-1* or *Mce1* genes for each dataset to identify conditions that phenocopy the bacterial requirement for these genes during vaccination (Fig. 2b). As expected, *Esx-1* genes are essential in wild-type C57BL/6 mice as compared to the *in vitro* selected input library (Fig. 2b), consistent with our data (Supplementary Fig. 3b). *Esx-1* genes become even more essential in immune-deficient mice, including Rag, NOS, IFN $\gamma$ , and Phox (Cybb) knock-out backgrounds. By contrast, conditions where *Esx-1* is not essential include *in vitro* hypoxia, *in vitro* acid stress, and *in vitro* amino acid limitation.

Across this same set of MtbTnDb conditions, we observed that *Mce1* genes are not required when grown *in vitro* in media where cholesterol is the sole carbon source, consistent with the known role of *Mce1* as a fatty-acid importer<sup>35,36</sup> (Fig. 2b). This suggests that bacteria surviving the immune pressure of vaccination have distinct metabolic activity or access to different nutrient sources. Overall, the rank order of conditions for *Mce1* genes is similar to that for genes in the *Esx-1* system. Like *Esx-1*, *Mce1* genes are less essential under *in vitro* hypoxia, *in vitro* acid stress, and *in vitro* amino acid limitation, and more essential in Rag, NOS, IFN $\gamma$ , and Phox knock-out mice (Fig. 2b). Because bacterial replication is uncontrolled in these immune-deficient mouse backgrounds but restricted under the aforementioned *in vitro* stress conditions, we hypothesized that *Esx-1* and *Mce1* may be required for rapid bacterial growth.

To test this hypothesis, we analyzed a large, published dataset of bacterial burden and TnSeq measurements collected across a panel of genetically diverse mice with variable capacity for *Mtb* control<sup>17</sup>. We evaluated the relationship between the essentiality of *Esx-1* and *Mce1* genes, indicated by the average  $\log_2$  fold-change in transposon insertion count in each gene set relative to the input library, and bacterial proliferation, reflected by endpoint CFU, across these mouse backgrounds. We found bacterial burden to be negatively correlated with the  $\log_2$  fold-change in transposon count for both *Esx-1* genes ( $r = -0.48$ ) and *Mce1* genes ( $r = -0.66$ ) (Fig. 2c, Supplementary Data 3). This is consistent with a model in which the *Esx-1* and *Mce1* systems are required under conditions of rapid bacterial replication, and the decreased essentiality of these genes in BCG-vaccinated mice may reflect a slow- or non-replicating state of the surviving bacteria.

### Differential effect of immunization strategy on the essentiality of *Esx-1* and *Mce1*

Given the poor performance of BCG in conferring lasting, protective immunity against *Mtb* infection and disease, significant efforts have been devoted toward the development of improved vaccine strategies. These

include subunit vaccines, novel attenuated whole cell vaccines, and methods of delivery that promise to enhance the immune response, including mucosal and intravenous routes of administration<sup>7,49</sup>. Quantitative and qualitative differences in immune response and degree and duration of protection have been described under various vaccination strategies<sup>49,50</sup>, yet bacterial physiology under these conditions has not been interrogated.

We therefore expanded our vaccine TnSeq challenge model to include additional immunization conditions (Fig. 3a). We included mice vaccinated with BCG via intravenous route (BCG-IV), which has been shown to confer substantially greater protection against *Mtb* compared to BCG-SQ in non-human primates<sup>51,52</sup>. This improvement in protection has been attributed to greater numbers of antigen-specific T cells as well as an enhanced humoral response<sup>51,53–55</sup>. In C57BL/6 mice, BCG-IV has not been shown to provide enhanced protection compared to BCG-SQ<sup>22,23</sup>, but has been found to induce qualitative differences in immune response, with a role for trained immunity found in some, but not all studies<sup>22,56</sup>. We also included mice vaccinated with a live, attenuated vaccine strain of *Mtb*,  $\Delta$ LprG, which has been shown to confer greater protection against *Mtb* than subcutaneous BCG (BCG-SQ) in the C3HeB/FeJ mouse model of infection, induce a more robust cytokine response, and elicit a polyfunctional CD4<sup>+</sup> T-cell response<sup>21,57</sup>. Finally, we included mice that had been infected via the aerosol route with H37Rv, then cured with combination antibiotic therapy (*Mtb*+cure). This approximates reinfection in humans and may provide insight into how *Mtb* escapes the immunity conferred by natural infection. A meta-analysis of epidemiological studies from the pre-antibiotic era found that prior *Mtb* infection confers a degree of protection against TB disease similar to that of BCG vaccination<sup>58</sup>. In mouse models, prior *Mtb* infection and cure confer approximately a log reduction in *Mtb* burden, similar to the level of protection afforded by subcutaneous BCG vaccination, the traditional benchmark for TB vaccine evaluation in pre-clinical animal models<sup>59,60</sup>.

Mice in each of these groups were challenged with the H37Rv transposon library, and surviving mutants were recovered and sequenced as described above. We found that bacterial burden was reduced by  $\sim 1.5$  logs in each arm of the experiment compared to naïve animals and was not significantly different across arms in the spleen, the site of transposon library selection (Supplementary Fig. 1c). While this suggests quantitatively similar selective pressure across the immunization strategies, we wanted to assess whether there were qualitative differences among these conditions as reflected by the bacterial genes essential for growth. Given the striking difference in essentiality of *Esx-1* and *Mce1* genes in BCG-SQ vaccinated compared to naïve animals, we first evaluated the essentiality of these systems.

Compared to naïve mice, many genes in the *Esx-1* and *Mce1* loci were significantly less essential in the  $\Delta$ LprG, BCG-IV, and *Mtb*+cure arms, consistent with our observations in BCG-SQ vaccinated animals (Fig. 3b, Supplementary Data 1). However, there are quantitative differences in the essentiality of these genes across the vaccination strategies. When transposon read counts are averaged across all genes in the *Esx-1* system, there is a significant difference among the vaccine strategies at both time points ( $p = 0.0001$  at 2 weeks,  $p = 0.0013$  at 4 weeks, Friedman test). There is a greater  $\log_2$  fold-change value for the BCG-SQ arm compared to *Mtb*+cure (2 weeks) and BCG-IV and *Mtb*+cure (4 weeks), indicating that *Esx-1* genes are less required in BCG-SQ vaccinated animals compared to other immune animals (Fig. 3c). Across genes in the *Mce1* system, there is also a significant difference in essentiality by condition ( $p < 0.0001$  at 2 weeks,  $p = 0.0012$  at 4 weeks, Friedman test). A similar trend was seen with *Mce1* as for *Esx-1*, with a significantly greater increase in transposon counts in BCG-SQ as compared to *Mtb*+cure (Fig. 3c). Thus, despite the similar degree of protection conferred by our immunization strategies, there are quantitative differences among the surviving bacterial transposon mutants, highlighting the potential for TnSeq to uncover unique bacterial genetic requirements under distinct immune conditions.

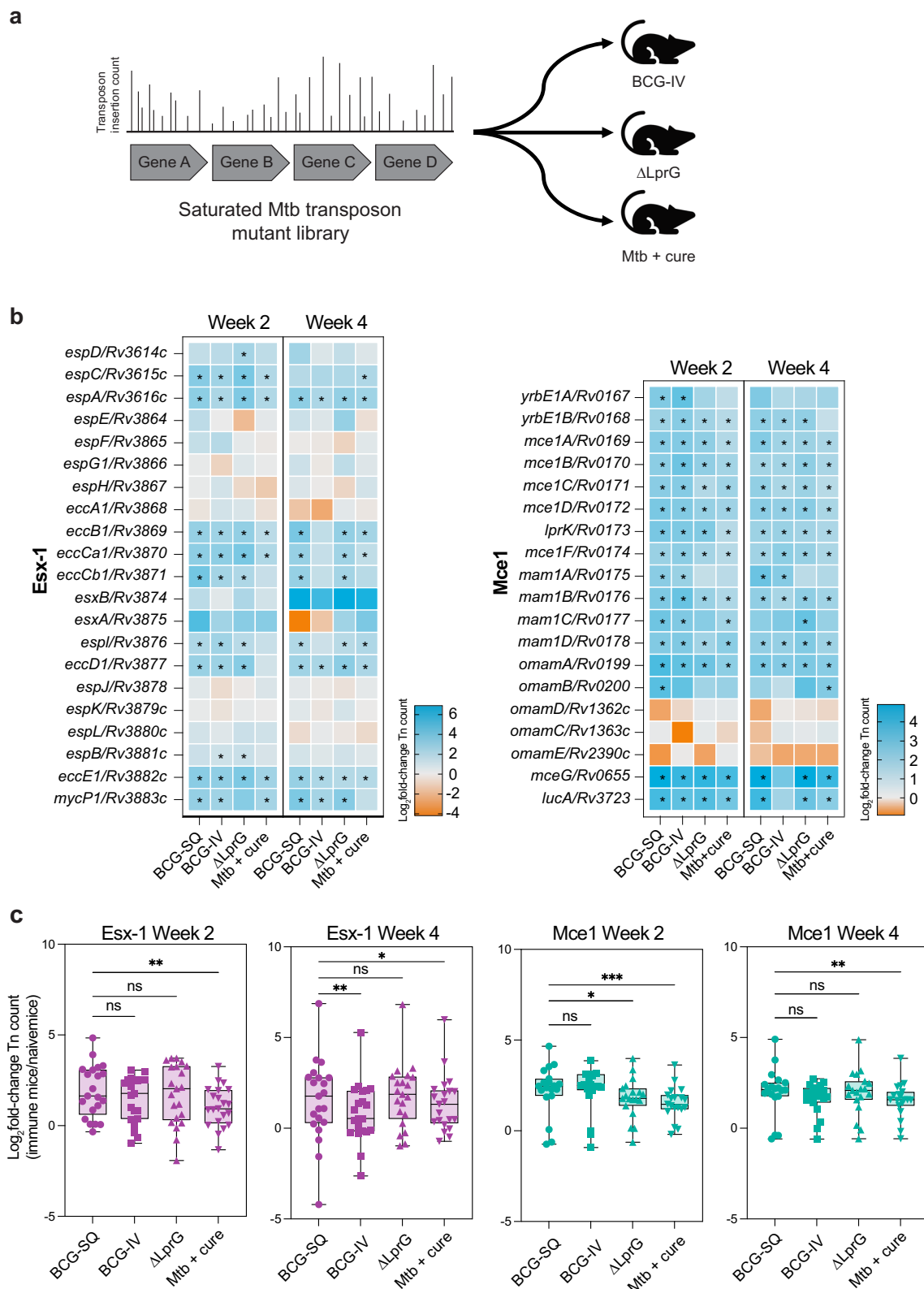


**Fig. 3 | Genetic requirements across distinct immunization conditions.**

**a** Experimental strategy for the expanded TnSeq screen.  $n = 2-5$  mice per group.

**b** Heatmaps showing log<sub>2</sub> fold-change in transposon insertion count relative to naïve mice for the Esx-1 genes (left panels) and Mce1 genes (right panels) for each immunization condition. Asterisks indicate adj.  $p < 0.05$  by the Transit resampling

pipeline, as detailed in the “Methods.” **c** Box plots showing log<sub>2</sub> fold-change in transposon insertion count for Esx-1 and Mce1 genes, relative to naïve mice. Significance determined by the Friedman test with Dunn’s multiple comparison to the BCG-SQ condition.

## Distinct immunization strategies impose differential selective pressures

Given the differences in essentiality of *Esx-1* and *Mce1* genes across vaccine conditions, we wanted to more comprehensively evaluate how memory responses induced by distinct immunization strategies impact bacterial genetic requirements. In each immune condition, between 4 and 41 genes were conditionally more essential, while between 23 and 61 genes were conditionally less essential (Supplementary Data 1). The less essential genes were highly overlapping across conditions (Fig. 4a), and the overlap set was largely comprised of genes in the *Esx-1* and *Mce1* systems (17/23 genes at 2 weeks, 12/14 genes at 4 weeks, Supplementary Fig. 4a). Beyond *Esx-1* and *Mce1* genes, six additional genes were less essential in all conditions at the 2-week time point, including the non-ribosomal peptide synthetase *nrp/Rv0101*; *pitA/Rv0545c*, a low-affinity phosphate importer; *Rv0485*, which regulates a PE/PPE pair; the biotin synthesis gene *bioA/Rv1568*; *cpsA/Rv3484*; and *satS/Rv3311*, a protein export chaperone<sup>61</sup>. At 4 weeks, in addition to the *Esx-1* and *Mce1* genes, *nrp/Rv0101* and *satS/Rv3311* remain significantly less essential. Overall, genes that were uniquely less essential in one condition had transposon insertion count  $\log_2$  fold-change values that trended in the same direction across the other immune conditions, but did not meet criteria for significance, resulting in high correlation coefficients across these genes (Supplementary Fig. 4b, c). Together, this suggests a conserved signature in the conditionally non-essential genes under memory immunity, driven by the decreased requirement for the key virulence pathways encoded by *Esx-1* and *Mce1* genes and other genes known to be essential during acute infection, including *cpsA/Rv3484* and *nrp/Rv0101*<sup>62,63</sup>. However, as shown in UpSet plots, there is greater variability in the genes that are significantly more essential under individual immune conditions (Fig. 4a). When the set of genes that are more essential in at least one condition are considered, the correlation coefficients among the  $\log_2$  fold-change values are lower than for the genes that are less essential (Supplementary Fig. 4d, e). This suggests that the immune pressures experienced by the bacteria may vary by immunization strategy.

While resampling provides a rigorous way to identify genes with statistically significant differences in transposon insertion count, a limitation of this approach is that genes that are close to, but do not meet, thresholds for statistical significance are not considered. We have previously demonstrated that quantitative differences in transposon insertion count are predictive of differences in mycobacterial physiology, even if a threshold for statistical significance is not met<sup>11</sup>. Therefore, to gain more biological insight into our data, we performed gene set enrichment analysis (GSEA) using the pre-ranked method, ranking all genes from each immunization arm of the study by the  $\log_2$  fold-change in transposon count relative to naïve animals. We then created gene sets from the defined in vitro stress conditions from MtbTnDb presented in Fig. 2b, where each set is comprised of genes that are significantly more or less essential under each in vitro condition, and looked for enrichment of these sets in our ranked data.

This analysis finds that for some in vitro conditions, the immune conditions have similar gene essentiality profiles, as indicated by a similar normalized enrichment score (NES) (Fig. 4b). For example, all immune conditions have a positive NES of similar magnitude for the gene sets more essential for growth in cholesterol media and in minimal media, indicating that genes essential for growth in these conditions are not required by the bacterium under immune memory. This suggests that the metabolic milieu experienced by Mtb is similar across immune conditions.

By contrast, for many of the in vitro stress conditions, including acid stress, hypoxia, iron limitation, nitrosative stress, and amino acid starvation, the NES varies both quantitatively and qualitatively (i.e., positive vs. negative enrichment) across immune conditions and over time. For example, genes that are more essential under in vitro nitrosative stress are more essential in BCG-SQ vaccinated mice and Mtb+cure mice, as indicated by a large, negative NES at the 2-week time point. However, the NES for this same gene set is less negative in  $\Delta$ LprG vaccinated mice and slightly positive in BCG-IV vaccinated animals at this time point. Comparing the 2- and 4-week time points, the NES for the nitrosative stress gene sets becomes less negative in

BCG-SQ vaccinated mice, suggesting a reduction in nitrosative stress over time, and flips from negative to positive in Mtb+cure animals, suggesting an absence of nitrosative stress in this immune condition. Taken together, this analysis suggests that TnSeq can provide insight into how different immunization strategies achieve bacterial control.

## Discussion

Tuberculosis will remain a global health emergency until a more effective vaccine is available. In the quest to develop an improved TB vaccine, numerous studies have characterized the host response to BCG and new vaccine candidates. Despite intensive study, immune correlates of protection remain elusive, and the features that determine bacterial control are incompletely characterized. Here, we have investigated this question from the bacterial perspective, using a functional genomics approach to interrogate bacterial physiology under the selective pressure of adaptive immunity induced by vaccination or previous infection.

Notably, we found that genes encoding the canonical virulence factors *Esx-1* and *Mce1* are less essential in mice with immunity induced by vaccination or prior Mtb infection. *Esx-1* is critical to establishing infection, playing myriad roles including inhibition of phagosome-lysosome fusion; phagolysosomal permeabilization and subsequent stimulation of Type I interferons via the cGAS-STING pathway and inflammasome activation via NLRP3; and recruitment of macrophages to form the nascent granuloma, providing a niche for bacterial replication<sup>38,44,64,65</sup>. The importance of these, and other, functions of *Esx-1* in Mtb pathogenesis is illustrated by BCG, which is avirulent because it lacks *Esx-1* due to a large genomic deletion<sup>66,67</sup>. The *Esx-1* secreted proteins ESAT-6 and CFP-10, encoded by *esxA/Rv3875* and *esxB/Rv3874*, respectively, in addition to being virulence determinants, are immunodominant antigens in mice and people. We therefore considered whether the relative advantage of *Esx-1* transposon mutants in BCG-vaccinated mice could reflect a lack of antigenic selection, since these genes are absent in BCG. However, our finding that *Esx-1* genes are also less essential in mice vaccinated with the  $\Delta$ LprG strain, which possesses an intact *Esx-1* system, and in mice previously infected with wild-type H37Rv is not consistent with antigenic escape. Rather, our data suggest that one or more of the physiologic roles fulfilled by the *Esx-1* system are no longer required in hosts with adaptive immunity.

Many of the roles played by *Esx-1* are critical during the initial stages of infection, hinting that vaccination or prior infection recapitulates some aspects of the post-primary infectious milieu, when *Esx-1* is no longer needed. Consistent with this interpretation, *Mce1* is also important during the early stages of infection. *Mce1* was identified as essential during acute Mtb infection in the first in vivo transposon mutagenesis study by Sassetti et al.<sup>9</sup>. In this seminal work, it was found that the growth defect of *Mce1* transposon mutants resolved later in infection, when *Mce4* genes, which encode a cholesterol import system, became essential. This led to the model, since experimentally validated, that Mtb consumes fatty acids during acute infection and switches to cholesterol as a nutrient source during chronic infection<sup>68,69</sup>. In our studies, we did not find a concomitant increase in the essentiality of *Mce4* genes in vaccinated mice. In agreement with our data, a TnSeq study using a BCG transposon library to challenge BCG-vaccinated cattle also found that genes in the *Mce1* system are less essential in the context of vaccination, but did not observe an increase in the essentiality of *Mce4* genes<sup>70</sup>. These observations suggest that bacteria surviving the memory immune response may utilize a nutrient source other than cholesterol, or may enter a slowly replicating state where nutritional demands are reduced.

It is known that the efficacy of antibiotics against Mtb is limited by the bacterium's ability to enter a slow-growing, persistent state<sup>71–73</sup>. Evidence suggests that persistent bacteria are also capable of evading the immune response during chronic infection<sup>74</sup>, and recent work employing a ribosomal RNA-based metric of bacterial replication indicates that BCG vaccination induces more rapid bacterial growth arrest<sup>75</sup>. Consistent with the model that bacteria surviving the immune memory response exist in a slow-growing state, our analyses of data from diverse in vitro and in vivo Mtb TnSeq

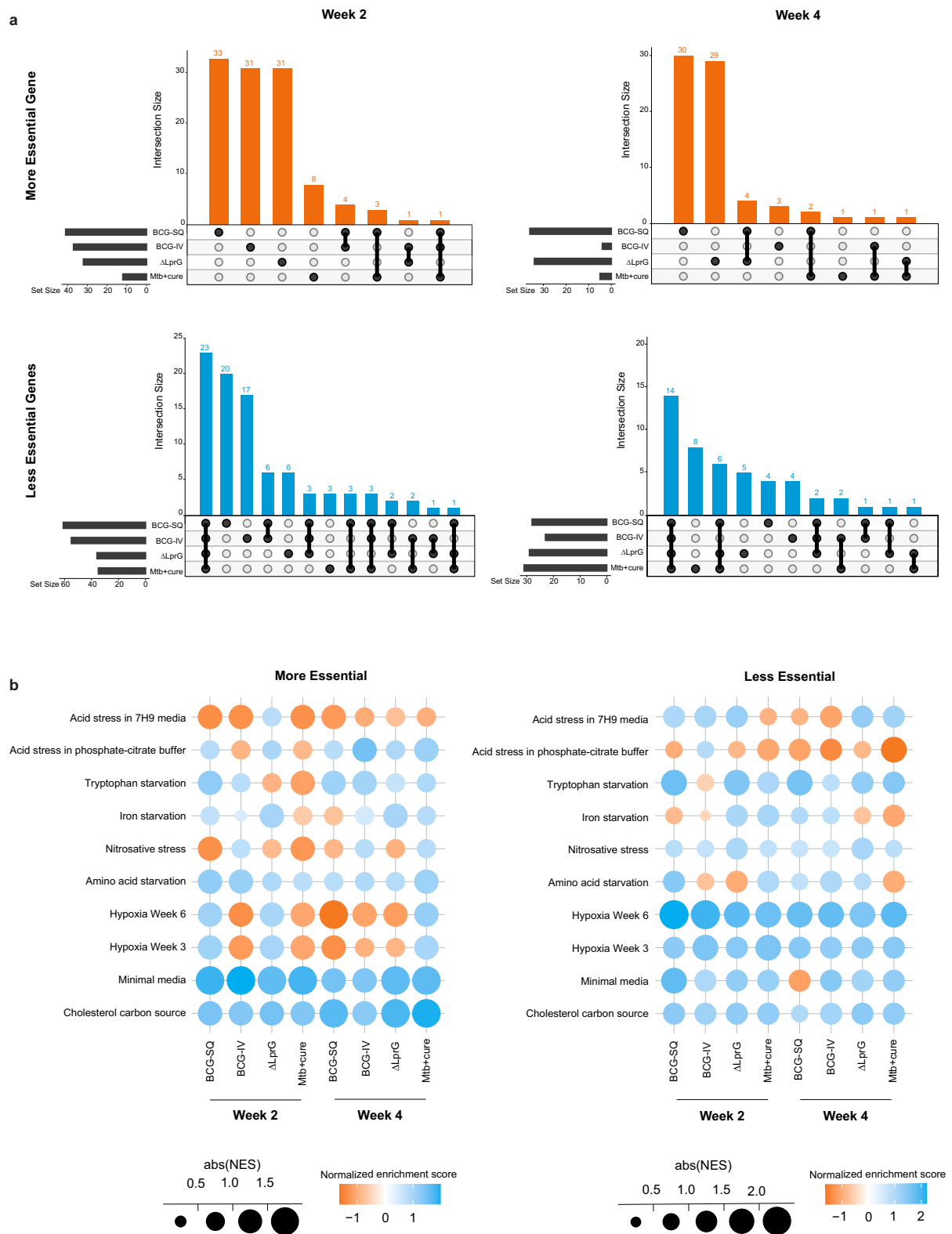


**Fig. 4 | Pathway analysis of differentially essential genes under immune memory conditions.** **a** UpSet plots of more essential genes in each immunization condition relative to naïve mice (upper panels) and less essential genes in each immunization condition relative to naïve mice (lower panels). **b** Bubble heatmaps of GSEA analysis of differentially essential genes. Each bubble represents the enrichment of a gene set,

defined by significantly more essential or less essential genes from an in vitro condition in MtbTnDb, against the ranked list of  $\log_2$ (fold-change) ratio of the TnSeq immunization condition using the GSEA preranked tool. The size of the bubble corresponds to the normalized enrichment score (NES); blue bubbles have a positive NES, and orange bubbles have a negative NES.



studies found that conditions of restricted bacterial growth most closely phenocopy the reduced requirement for *Esx-1* and *Mce1* genes we observed in immunized mice. This agrees with a BCG transposon mutagenesis study conducted in a chemostat, a bioreactor capable of controlling bacterial growth rate via regulated inflow and outflow of media, which found that *Mce1* genes become non-essential under conditions of slow growth, although the essentiality of *Esx-1* genes could not be assessed because BCG lacks an intact *Esx-1* system<sup>76</sup>. Intriguingly, our data may also suggest a functional link between *Mce1* and *Esx-1*, consistent with comparative genomic analyses<sup>77</sup>. A plausible model for such a relationship could be that *Esx-1*, which permeabilizes the phagolysosomal membrane<sup>78–80</sup>, facilitates access to the host-derived fatty acids imported by *Mce1*. This nutrient acquisition may be most critical under conditions of rapid bacterial replication, and less essential when the bacterial growth rate is reduced.

Immune correlates of protection following *Mtb* infection and in the context of vaccination are still lacking<sup>50</sup>. A key finding of this work is that different vaccination strategies induce qualitatively distinct bacterial genetic requirements for survival, and these are different from the bacterial requirements to survive immunity conferred by prior *Mtb* infection. We interpret the differences in bacterial genetic requirements to reflect differences in immune pressures imposed by each immunization strategy. Currently, the pipeline for TB vaccine development includes a number of candidate LAV<sup>7,49,81</sup>, with MTBVAC being the most advanced in human clinical trials. Emerging data suggest that there are differences in the immunogenicity and efficacy of different mycobacterial LAV<sup>82</sup>. For example, it has been shown that BCG and  $\Delta$ LprG induce different levels of antigen-specific T cells following vaccination in mice<sup>21</sup>. In particular,  $\Delta$ LprG, which is more effective than BCG, was shown to induce more polyfunctional CD4+ T lymphocyte responses. Our data support the notion that LAV will also differentially sculpt the subsequent immunological pressures on the bacterium.

A limitation of this work is that we investigated only one vaccine modality, LAV, and we did not systematically investigate the effect of vaccination route. Future studies are needed to determine whether other vaccine modalities, including vectored vaccines and mRNA vaccines, or alternative administration routes, such as intravenous or mucosal vaccination, also differentially impact *Mtb* physiology. Additional studies on the timing of induction of specific immune cell subsets under various vaccine conditions in conjunction with TnSeq may further our understanding of which mycobacterial genes are required to counter specific immune responses. Extended studies using targeted bacterial genetic mutants and reporter strains may further elucidate how *Mtb* persists in vaccinated hosts and help explain how and why reinfection occurs. In the long term, such studies may contribute to rational vaccine and adjuvant design.

An inherent limitation of TnSeq is that a high bacterial dose must be delivered via the lateral tail vein for selection in the spleen. This dose and route of delivery is necessitated by the complex pool of over 50,000 individual transposon mutants that would be bottlenecked by a more physiologic dose delivered aerogenically. However, several studies have shown that genetic requirements identified by TnSeq are generally confirmed in aerosol route infections<sup>13,16,17,83</sup>. Another limitation of TnSeq is that simultaneously profiling host immune responses at the site of infection is not possible because the tissues are required for bacterial outgrowth and transposon-junction sequencing. Future studies evaluating longitudinal peripheral immune responses, including immune cell profiling, serum cytokine measurements, and antibody responses, may provide additional insight. Integrated with TnSeq data, such studies may identify the specific effector mechanisms that contribute to the control of *Mtb*. Performing TnSeq studies in vaccinated knock-out mice or mice treated with blocking antibodies to diminish the activity of critical arms of the adaptive immune response, such as CD4+ and CD8+ T lymphocytes or immune signaling, may further elucidate key bacterial virulence mechanisms that have evolved to counter these immune pressures.

Altogether, this work highlights the utility of functional genetic screens such as TnSeq under vaccine conditions to identify bacterial vulnerabilities

that could be targeted in vaccine design. This approach, when applied across diverse vaccination modalities, *Mtb* challenge strains, and host genetic backgrounds, may further illuminate the complexities of bacterial evasion of host immune responses and inform the development of more effective vaccines for tuberculosis.

## Methods

### Bacterial strains

Unless otherwise noted, *Mtb* was cultured in Middlebrook 7H9 salts supplemented with 10% oleic acid-albumin-dextrose-catalase (OADC), 0.5% glycerol, and 0.05% Tween 80 at 37 °C with agitation, or plated on 7H10 agar supplemented with 10% OADC, 0.5% glycerol, and 0.05% Tween 80 at 37 °C. The saturated H37Rv transposon library was previously generated<sup>11</sup> and outgrown on 7H10 agar supplemented with 10% OADC, 0.5% glycerol, 0.05% Tween 80, 0.2% Cas-amino acids (Difco), and 20 µg/mL kanamycin at 37 °C. BCG was obtained from the Statens Serum Institute and prepared as previously described<sup>21</sup>. The *Esx-1* mutant is a deletion strain of *esxA*/Rv3875 that disrupts the entire secretion system, and was generated as described<sup>46</sup>.

### Animals and infections

Six- to eight-week-old female C57BL/6 mice were purchased from Jackson Laboratories (Bar Harbor, ME). Infected animals were housed in Biosafety Level 3 facilities under specific-pathogen-free conditions at the Harvard T. H. Chan School of Public Health. The protocols, personnel, and animal use were approved and monitored by the Harvard University Institutional Animal Care and Use Committee.

For BCG-SQ and  $\Delta$ LprG vaccinations, animals were anesthetized with isoflurane using a precision vaporizer and induction chamber, then vaccinated by injecting 100 µL of frozen bacterial culture (2e7 CFU total) subcutaneously in the flank. For IV-BCG vaccination experiments, mice were briefly restrained in an IACUC-approved restraining tube, and 2e7 CFU of BCG in 100 µL were injected into the lateral tail vein. Mice were rested for 12 weeks post-vaccination prior to infection with the transposon library or single-strain infections. For aerosol infections, animals were infected with H37Rv using a Glas-Col instrument (Terra-Haute, Indiana) to deliver ~100 CFU. After 4 weeks of infection, *Mtb*+cure animals were treated with rifampicin (0.2 g/L) and isoniazid (0.1 g/L) in the drinking water for 7 weeks. The antibiotic-containing water was changed weekly. Animals were rested for 1 week to ensure no carry-over effects of antibiotic selection on the challenge transposon library. Transposon library infections were performed by injecting 2e6 CFU of frozen library in 100 µL in the lateral tail vein as described above. Single-strain infections with wild-type H37Rv or the *Esx-1* mutant were performed by injecting 2e6 CFU of mid-log bacterial culture in 100 µL in the lateral tail vein as described above. To recover tissue for CFU enumeration or transposon-junction sequencing, animals were euthanized with an overdose of isoflurane followed by cervical dislocation in accordance with the Harvard IACUC-approved protocol and AVMA guidelines for the Euthanasia of Animals: 2020 Edition.

### Transposon library sequencing and analysis

Spleens from infected animals were homogenized and plated to recover 1e6 CFU. After 3 weeks of outgrowth, colonies were scraped and genomic DNA extracted. Transposon-junction libraries were prepared from the recovered genomic DNA essentially as previously described<sup>11</sup>. Libraries were sequenced on a HiSeq 2500 at the Tufts University Genomics Core, with 100 bp paired-end reads. Read mapping and statistical comparisons of read counts between conditions were performed using Transit v3.2.7. Reads were normalized with the TTR method, insertions in the central 90% of each gene were considered, and a LOESS correction was performed. Repetitive regions, such as PE/PPE genes, were excluded as previously described<sup>11</sup>; excluded genes are listed in Supplementary Data 1.

## Data analysis

Statistical tests were performed with GraphPad Prism v10.3.0. Pathway enrichment analysis was performed with g:Profiler<sup>84</sup> using Sanger roles for functional annotation. The Sanger terms “IS1081,” “Phage related functions,” “PE\_PGRS subfamily,” “PE Subfamily,” “IS6110,” and “PPE family” were excluded from analysis, as were any genes excluded from Transit analysis, as detailed above. GSEA was performed using the preranked tool<sup>85</sup>. TnSeq datasets were downloaded from MtbTnDb.app on January 25, 2024, and conditions and references are included in Supplementary Data 2. Venn diagrams were generated with Deep Venn<sup>86</sup>.

## Data availability

Raw transposon-junction sequencing reads that support the findings of this study have been deposited to the NCBI Sequence Read Archive, BioProject accession number [PRJNA1183901](https://www.ncbi.nlm.nih.gov/bioproject/PRJNA1183901), and findings can be reproduced by performing the bioinformatic analyses described in “Methods.” All other data to support the findings of this work are located within the paper and the Supplementary files.

Received: 8 November 2024; Accepted: 30 April 2025;

Published online: 22 May 2025

## References

- World Health Organization. *Global Tuberculosis Report 2024* (World Health Organization, 2024).
- Lange, C. et al. 100 years of *Mycobacterium Bovis* Bacille Calmette-Guérin. *Lancet Infect. Dis.* **22**, e2–e12 (2022).
- Vergne, I., Chua, J., Singh, S. B. & Deretic, V. Cell biology of mycobacterium tuberculosis phagosome. *Annu. Rev. Cell Dev. Biol.* **20**, 367–394 (2004).
- Pishesha, N., Harmand, T. J. & Ploegh, H. L. A guide to antigen processing and presentation. *Nat. Rev. Immunol.* **22**, 751–764 (2022).
- Lu, Y.-J. et al. CD4 T cell help prevents CD8 T cell exhaustion and promotes control of *Mycobacterium tuberculosis* infection. *Cell Rep.* **36**, 109696 (2021).
- Carpenter, S. M., Yang, J. D., Lee, J., Barreira-Silva, P. & Behar, S. M. Vaccine-elicited memory CD4+ T cell expansion is impaired in the lungs during tuberculosis. *PLoS Pathog.* **13**, e1006704 (2017).
- Andersen, P. & Scriba, T. J. Moving tuberculosis vaccines from theory to practice. *Nat. Rev. Immunol.* **19**, 550–562 (2019).
- Sassetti, C. M., Boyd, D. H. & Rubin, E. J. Comprehensive identification of conditionally essential genes in mycobacteria. *Proc. Natl. Acad. Sci. USA* **98**, 12712–12717 (2001).
- Sassetti, C. M. & Rubin, E. J. Genetic requirements for mycobacterial survival during infection. *Proc. Natl. Acad. Sci. USA* **100**, 12989–12994 (2003).
- Zhang, Y. J. et al. Global assessment of genomic regions required for growth in *Mycobacterium tuberculosis*. *PLoS Pathog.* **8**, e1002946 (2012).
- Carey, A. F. et al. TnSeq of *Mycobacterium tuberculosis* clinical isolates reveals strain-specific antibiotic liabilities. *PLoS Pathog.* **14**, e1006939 (2018).
- Carey, A. F. et al. Multiplexed strain phenotyping defines consequences of genetic diversity in *Mycobacterium tuberculosis* for infection and vaccination outcomes. *mSystems* e0011022 <https://doi.org/10.1128/msystems.00110-22> (2022).
- Zhang, Y. J. et al. Tryptophan biosynthesis protects *Mycobacteria* from CD4 T-cell-mediated killing. *Cell* **155**, 1296–1308 (2013).
- Xu, W. et al. Chemical genetic interaction profiling reveals determinants of intrinsic antibiotic resistance in *Mycobacterium tuberculosis*. *Antimicrob. Agents Chemother.* **61**, <https://doi.org/10.1128/aac.01334-17> (2017).
- DeJesus, M. A. et al. Comprehensive essentiality analysis of the *Mycobacterium tuberculosis* genome via saturating transposon mutagenesis. *mBio* **8**, <https://doi.org/10.1128/mbio.02133-16> (2017).
- Bellerose, M. M. et al. Distinct bacterial pathways influence the efficacy of antibiotics against *Mycobacterium tuberculosis*. *mSystems* **5**, e00396–20 (2020).
- Smith, C. M. et al. Host-pathogen genetic interactions underlie tuberculosis susceptibility in genetically diverse mice. *eLife* **11**, e74419 (2022).
- Rengarajan, J., Bloom, B. R. & Rubin, E. J. Genome-wide requirements for *Mycobacterium tuberculosis* adaptation and survival in macrophages. *Proc. Natl. Acad. Sci. USA* **102**, 8327–8332 (2005).
- Block, A. M., Wiegert, P. C., Namugenyi, S. B. & Tischler, A. D. Transposon sequencing reveals metabolic pathways essential for *Mycobacterium tuberculosis* infection. *PLoS Pathog.* **20**, e1011663 (2023).
- Griffin, J. E. et al. High-resolution phenotypic profiling defines genes essential for mycobacterial growth and cholesterol catabolism. *PLoS Pathog.* **7**, e1002251 (2011).
- Martinot, A. J. et al. Protective efficacy of an attenuated *Mtb* ΔLprG vaccine in mice. *PLoS Pathog.* **16**, e1009096 (2020).
- Bickett, T. E. et al. Characterizing the BCG induced macrophage and neutrophil mechanisms for defense against *Mycobacterium tuberculosis*. *Front. Immunol.* **11**, 1202 (2020).
- Lefford, M. J. Induction and expression of immunity after BCG immunization. *Infect. Immun.* **18**, 646–653 (1977).
- Irwin, S. M. et al. Immune response induced by three *Mycobacterium bovis* BCG substrains with diverse regions of deletion in a C57BL/6 mouse model. *Clin. Vaccin. Immunol.* **15**, 750–756 (2008).
- Cadena, A. M. et al. Concurrent infection with *Mycobacterium tuberculosis* confers robust protection against secondary infection in macaques. *PLoS Pathog.* **14**, e1007305 (2018).
- DeJesus, M. A., Ambadipudi, C., Baker, R., Sassetti, C. & Iøerger, T. R. TRANSIT-A software tool for Himar1 TnSeq analysis. *PLoS Comput. Biol.* **11**, e1004401 (2015).
- Zhu, J.-H. et al. Rifampicin can induce antibiotic tolerance in mycobacteria via paradoxical changes in *rpoB* transcription. *Nat. Commun.* **9**, 4218 (2018).
- Iøerger, T. R. Analysis of gene essentiality from TnSeq data using transit. *Methods Mol. Biol.* **2377**, 391–421 (2022).
- Smith, C. M. et al. Tuberculosis susceptibility and vaccine protection are independently controlled by host genotype. *mBio* **7**, <https://doi.org/10.1128/mbio.01516-16> (2016).
- Beaucher, J. et al. Novel *Mycobacterium tuberculosis* anti-σ factor antagonists control σF activity by distinct mechanisms. *Mol. Microbiol.* **45**, 1527–1540 (2002).
- Mir, M. et al. *Mycobacterium* gene *cuvA* is required for optimal nutrient utilization and virulence. *Infect. Immun.* **82**, 4104–4117 (2014).
- Daniel, J., Sirakova, T. & Kolattukudy, P. An Acyl-CoA synthetase in *Mycobacterium tuberculosis* involved in triacylglycerol accumulation during dormancy. *PLoS ONE* **9**, e114877 (2014).
- Arroyo, L., Marín, D., Franken, K. L. M. C., Ottenhoff, T. H. M. & Barrera, L. F. Potential of DosR and Rpf antigens from *Mycobacterium tuberculosis* to discriminate between latent and active tuberculosis in a tuberculosis endemic population of Medellín Colombia. *BMC Infect. Dis.* **18**, 26 (2018).
- Goletti, D. et al. Response to Rv2628 latency antigen associates with cured tuberculosis and remote infection. *Eur. Respir. J.* **36**, 135–142 (2009).
- Nazarova, E. V. et al. The genetic requirements of fatty acid import by *Mycobacterium tuberculosis* within macrophages. *eLife* **8**, e43621 (2019).
- Nazarova, E. V. et al. Rv3723/LucA coordinates fatty acid and cholesterol uptake in *Mycobacterium tuberculosis*. *eLife* **6**, e26969 (2017).
- Fortune, S. M. et al. Mutually dependent secretion of proteins required for mycobacterial virulence. *Proc. Natl. Acad. Sci. USA* **102**, 10676–10681 (2005).

38. Stanley, S. A., Raghavan, S., Hwang, W. W. & Cox, J. S. Acute infection and macrophage subversion by *Mycobacterium tuberculosis* require a specialized secretion system. *Proc. Natl. Acad. Sci. USA* **100**, 13001–13006 (2003).
39. Brodin, P. et al. Dissection of ESAT-6 system 1 of *Mycobacterium tuberculosis* and impact on immunogenicity and virulence. *Infect. Immun.* **74**, 88–98 (2006).
40. Gröschel, M. I., Sayes, F., Simeone, R., Majlessi, L. & Brosch, R. ESX secretion systems: mycobacterial evolution to counter host immunity. *Nat. Rev. Microbiol.* **14**, 677–691 (2016).
41. MacGurn, J. A. & Cox, J. S. A genetic screen for *Mycobacterium tuberculosis* mutants defective for phagosome maturation arrest identifies components of the ESX-1 secretion system. *Infect. Immun.* **75**, 2668–2678 (2007).
42. McLaughlin, B. et al. A *Mycobacterium* ESX-1-secreted virulence factor with unique requirements for export. *PLoS Pathog.* **3**, e105 (2007).
43. Raghavan, S., Manzanillo, P., Chan, K., Dovey, C. & Cox, J. S. Secreted transcription factor controls *Mycobacterium tuberculosis* virulence. *Nature* **454**, 717–721 (2008).
44. Stanley, S. A., Johndrow, J. E., Manzanillo, P. & Cox, J. S. The type I IFN response to infection with *Mycobacterium tuberculosis* requires ESX-1-mediated secretion and contributes to pathogenesis. *J. Immunol.* **178**, 3143–3152 (2007).
45. de Jonge, M. I. et al. ESAT-6 from *Mycobacterium tuberculosis* dissociates from its putative chaperone CFP-10 under acidic conditions and exhibits membrane-lysing activity. *J. Bacteriol.* **189**, 6028–6034 (2007).
46. Guinn, K. M. et al. Individual RD1-region genes are required for export of ESAT-6/CFP-10 and for virulence of *Mycobacterium tuberculosis*. *Mol. Microbiol.* **51**, 359–370 (2004).
47. Lewis, K. N. et al. Deletion of RD1 from *Mycobacterium tuberculosis* mimics Bacille Calmette–Guérin attenuation. *J. Infect. Dis.* **187**, 117–123 (2003).
48. Jinich, A. et al. The *Mycobacterium tuberculosis* transposon sequencing database (MtbTnDB): a large-scale guide to genetic conditional essentiality. *bioRxiv* <https://doi.org/10.1101/2021.03.05.434127> (2024).
49. Scriba, T. J., Netea, M. G. & Ginsberg, A. M. Key recent advances in TB vaccine development and understanding of protective immune responses against *Mycobacterium tuberculosis*. *Semin. Immunol.* **50**, 101431 (2020).
50. Nemes, E. et al. The quest for vaccine-induced immune correlates of protection against tuberculosis. *Vaccin. Insights* **1**, 165–181 (2022).
51. Darrah, P. A. et al. Prevention of tuberculosis in macaques after intravenous BCG immunization. *Nature* **577**, 95–102 (2020).
52. Anacker, R. L. et al. Superiority of intravenously administered BCG and BCG cell walls in protecting rhesus monkeys (*Macaca mulatta*) against airborne tuberculosis. *Z. Fur Immun. Exp. Klin. Immunol.* **143**, 363–376 (1972).
53. Simonson, A. W. et al. Intravenous BCG-mediated protection against tuberculosis requires CD4<sup>+</sup> T cells and CD8 $\alpha$ <sup>+</sup> lymphocytes. *J. Exp. Med.* **222**, e20241571 (2025).
54. Irvine, E. B. et al. Robust IgM responses following intravenous vaccination with Bacille Calmette–Guérin associate with prevention of *Mycobacterium tuberculosis* infection in macaques. *Nat. Immunol.* **22**, 1515–1523 (2021).
55. Irvine, E. B. et al. Humoral correlates of protection against *Mycobacterium tuberculosis* following intravenous BCG vaccination in rhesus macaques. *iScience* **27**, 111128 (2024).
56. Kaufmann, E. et al. BCG educates hematopoietic stem cells to generate protective innate immunity against tuberculosis. *Cell* **172**, 176–190.e19 (2018).
57. Martinot, A. J. et al. Mycobacterial Metabolic Syndrome: LprG and Rv1410 regulate triacylglyceride levels, growth rate and virulence in *Mycobacterium tuberculosis*. *PLoS Pathog.* **12**, e1005351 (2016).
58. Martinez, L. et al. Infant BCG vaccination and risk of pulmonary and extrapulmonary tuberculosis throughout the life course: a systematic review and individual participant data meta-analysis. *Lancet Glob. Health* **10**, e1307–e1316 (2022).
59. Jung, Y.-J., Ryan, L., LaCourse, R. & North, R. J. Properties and protective value of the secondary versus primary T helper type 1 response to airborne *Mycobacterium tuberculosis* infection in mice. *J. Exp. Med.* **201**, 1915–1924 (2005).
60. Mollenkopf, H.-J., Kursar, M. & Kaufmann, S. H. E. Immune response to postprimary tuberculosis in mice: *Mycobacterium tuberculosis* and *Mycobacterium Bovis* Bacille Calmette–Guérin induce equal protection. *J. Infect. Dis.* **190**, 588–597 (2004).
61. Miller, B. K. et al. *Mycobacterium tuberculosis* SatS is a chaperone for the SecA2 protein export pathway. *eLife* **8**, e40063 (2019).
62. Grigsby, S. J. et al. CpsA mediates infection of recruited lung myeloid cells by *Mycobacterium tuberculosis*. *Cell Rep.* **43**, 114201 (2024).
63. Bhatt, K. et al. A nonribosomal peptide synthase gene driving virulence in *Mycobacterium tuberculosis*. *mSphere* **3**, e00352-18 (2018).
64. Davis, J. M. & Ramakrishnan, L. The role of the granuloma in expansion and dissemination of early tuberculous infection. *Cell* **136**, 37–49 (2009).
65. Wong, K. & Jacobs, W. R. Jr. Critical role for NLRP3 in necrotic death triggered by *Mycobacterium tuberculosis*. *Cell. Microbiol.* **13**, 1371–1384 (2011).
66. Behr, M. A. et al. Comparative genomics of BCG vaccines by whole-genome DNA microarray. *Science* **284**, 1520–1523 (1999).
67. Pym, A. S., Brodin, P., Brosch, R., Huerre, M. & Cole, S. T. Loss of RD1 contributed to the attenuation of the live tuberculosis vaccines *Mycobacterium bovis* BCG and *Mycobacterium microti*. *Mol. Microbiol.* **46**, 709–717 (2002).
68. Pandey, A. K. & Sassetti, C. M. Mycobacterial persistence requires the utilization of host cholesterol. *Proc. Natl. Acad. Sci. USA* **105**, 4376–4380 (2008).
69. Lovewell, R. R., Sassetti, C. M. & VanderVen, B. C. Chewing the fat: lipid metabolism and homeostasis during *M. tuberculosis* infection. *Curr. Opin. Microbiol.* **29**, 30–36 (2016).
70. Smith, A. A. et al. Genetic screening for the protective antigenic targets of BCG vaccination. *Tuberculosis* **124**, 101979 (2020).
71. Dhar, N. & McKinney, J. D. *Mycobacterium tuberculosis* persistence mutants identified by screening in isoniazid-treated mice. *Proc. Natl. Acad. Sci. USA* **107**, 12275–12280 (2010).
72. Vilchèze, C. et al. Enhanced respiration prevents drug tolerance and drug resistance in *Mycobacterium tuberculosis*. *Proc. Natl. Acad. Sci. USA* **114**, 4495–4500 (2017).
73. Sebastian, J. et al. Origin and dynamics of *Mycobacterium tuberculosis* subpopulations that predictably generate drug tolerance and resistance. *mBio* **13**, e02795-22 (2022).
74. Muñoz-Eliás, E. J. et al. Replication dynamics of *Mycobacterium tuberculosis* in chronically infected mice. *Infect. Immun.* **73**, 546–551 (2005).
75. Cooper, S. K. et al. Heterogeneity in immune cell composition is associated with *Mycobacterium tuberculosis* replication at the granuloma level. *Front. Immunol.* **15**, 1427472 (2024).
76. Beste, D. J. V. et al. The genetic requirements for fast and slow growth in mycobacteria. *PLoS ONE* **4**, e5349 (2009).
77. Das, C., Ghosh, T. S. & Mande, S. S. Computational analysis of the ESX-1 region of *Mycobacterium tuberculosis*: insights into the mechanism of type VII secretion system. *PLoS ONE* **6**, e27980 (2011).
78. Conrad, W. H. et al. Mycobacterial ESX-1 secretion system mediates host cell lysis through bacterium contact-dependent gross membrane disruptions. *Proc. Natl. Acad. Sci. USA* **114**, 1371–1376 (2017).
79. Wel, et al. M. tuberculosis and M. leprae translocate from the phagolysosome to the cytosol in myeloid cells. *Cell* **129**, 1287–1298 (2007).

80. Smith, J. et al. Evidence for pore formation in host cell membranes by ESX-1-secreted ESAT-6 and its role in *Mycobacterium marinum* escape from the vacuole. *Infect. Immun.* **76**, 5478–5487 (2008).
81. Flores-Valdez, M. A., Kupz, A. & Subbian, S. Recent developments in *Mycobacteria*-based live attenuated vaccine candidates for tuberculosis. *Biomedicines* **10**, 2749 (2022).
82. Muruganandah, V. et al. A systematic approach to simultaneously evaluate safety, immunogenicity, and efficacy of novel tuberculosis vaccination strategies. *Sci. Adv.* **6**, eaaz1767 (2020).
83. Nambi, S. et al. The oxidative stress network of *Mycobacterium tuberculosis* reveals coordination between radical detoxification systems. *Cell Host Microbe* **17**, 829–837 (2015).
84. Kolberg, L. et al. g:Profiler—interoperable web service for functional enrichment analysis and gene identifier mapping (2023 update). *Nucleic Acids Res.* **51**, W207–W212 (2023).
85. Subramanian, A. et al. Gene set enrichment analysis: a knowledge-based approach for interpreting genome-wide expression profiles. *Proc. Natl. Acad. Sci. USA* **102**, 15545–15550 (2005).
86. Hulsen T. DeepVenn—a web application for the creation of area-proportional Venn diagrams using the deep learning framework Tensorflow.js. *Arxiv* <https://doi.org/10.48550/arxiv.2210.04597> (2022).

## Acknowledgements

We thank Larry Pipkin and Noman Siddiqi, who manage the Harvard T.H. Chan School of Public Health BSL-3 facilities; Shoko Wakabayashi, Jaimie Sixsmith, and Xin Wang for assistance with BSL-3 experiments; members of the Fortune, Rubin, and Bryson labs for feedback and thoughtful discussions. The support and resources from the Center for High Performance Computing at the University of Utah are gratefully acknowledged.

## Author contributions

Conception and design: A.J.M. and A.F.C. Performing of experiments: A.F.C., A.J.M., N.J. Data acquisition: A.F.C. and A.J.M. Analysis and interpretation of data: K.S.J., K.W., N.C., T.R.I., A.J.M., A.F.C. Manuscript preparation and revisions: K.S.J., S.M.F., T.R.I., A.J.M., A.F.C. Study

supervision: S.M.F., A.J.M., A.F.C. All authors reviewed and approved the manuscript.

## Competing interests

The authors declare no competing interests.

## Additional information

**Supplementary information** The online version contains supplementary material available at <https://doi.org/10.1038/s41541-025-01150-9>.

**Correspondence** and requests for materials should be addressed to Amanda J. Martinot or Allison F. Carey.

**Reprints and permissions information** is available at <http://www.nature.com/reprints>

**Publisher's note** Springer Nature remains neutral with regard to jurisdictional claims in published maps and institutional affiliations.

**Open Access** This article is licensed under a Creative Commons Attribution-NonCommercial-NoDerivatives 4.0 International License, which permits any non-commercial use, sharing, distribution and reproduction in any medium or format, as long as you give appropriate credit to the original author(s) and the source, provide a link to the Creative Commons licence, and indicate if you modified the licensed material. You do not have permission under this licence to share adapted material derived from this article or parts of it. The images or other third party material in this article are included in the article's Creative Commons licence, unless indicated otherwise in a credit line to the material. If material is not included in the article's Creative Commons licence and your intended use is not permitted by statutory regulation or exceeds the permitted use, you will need to obtain permission directly from the copyright holder. To view a copy of this licence, visit <http://creativecommons.org/licenses/by-nc-nd/4.0/>.

© The Author(s) 2025